JACS
JOURNAL OF THE AMERICAN CHEMICAL SOCIETY
Article
pubs.acs.org/JACS

Mechanistic Insights into the Hydrolysis of a Nucleoside Triphosphate Model in Neutral and Acidic Solution

Rachel Glaves,* Gerald Mathias,† and Dominik Marx

Lehrstuhl für Theoretische Chemie, Ruhr-Universität Bochum, 44780 Bochum, Germany

Supporting Information

ABSTRACT: Nucleoside triphosphate hydrolysis is an essential component of all living systems. Despite extensive research, the exact modus and mechanism of this ubiquitous reaction still remain elusive. In this work, we examined the detailed hydrolysis mechanisms of a model nucleoside triphosphate in acidic and neutral solution by means of *ab initio* simulations. The timescale of the reaction was accessed through use of an accelerated sampling method, metadynamics. Both hydrolyses were found to proceed via different mechanisms; the acidic system reacted by means of concerted general acid catalysis (found to be a so-called $D_NA_NA_HD_{xh}$ mechanism), whereas the neutral system reacted by way of a different mechanism (namely, $D_N{*}A_ND_{xh}A_H$). A neighboring water molecule took on the role of a general base in both systems, which has not been seen before but is a highly plausible reaction path, meaning that substrate-assisted catalysis was not observed in the bulk water environment.

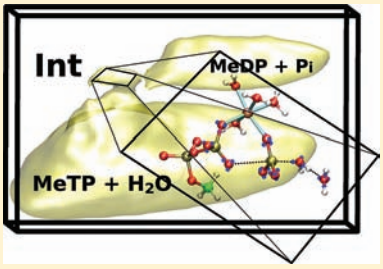

INTRODUCTION

The hydrolysis of nucleoside triphosphates such as guanosine triphosphate (GTP) plays an essential part in the biochemistry of living organisms. The catalysis of this one unique reaction by various enzymes leads to a myriad of different functions such as muscle contraction, replication of genetic material, and signal transmission.[1,2] It is, therefore, hardly surprising that the underlying reaction of phosphoester hydrolysis has been the subject of intense experimental and theoretical studies *in vacuo* and in solution; see refs 3−23 and references within, to name but a few. Despite these efforts, a complete picture of the reaction mechanism, including the nature of the transition state (TS) in particular, has not yet been obtained, and thus, this universal reaction still remains a controversial puzzle. In this study, we have investigated the hydrolysis of a methylated triphosphate (MeTP) molecule solvated in bulk water at ambient conditions. The entire system was treated at the same electronic structure level and enhanced sampling *ab initio* simulations were employed to include thermal fluctuations and entropic effects. The results reveal an unexpectedly complex picture for what one would expect to be a simple hydrolysis reaction in terms of multidimensional free energy surfaces (FES) and detailed reaction mechanisms, which are seen to be sensitive to pH conditions and involve solvent assistance in a nontrival fashion.

According to the literature,[3,4,7,14,18] the mechanism of phosphate hydrolysis can occur through either a dissociative or an associative TS depending on the bonding pattern to the incoming nucleophile and the leaving group. In the dissociative or S_N1 limit, the leaving group departs before nucleophilic attack, whereas in the (concerted) associative or S_N2 limit, the nucleophile attacks prior to leaving group bond cleavage. Furthermore, these reaction mechanisms can be either concerted or stepwise, depending on whether a stable intermediate is formed on the FES in the course of the reaction. The essential difference between the two limiting cases is a shift from the formation of a stable intermediate in the dissociative ($D_N + A_N$) borderline case to merely a TS in the concerted associative (A_ND_N) borderline case. Another pathway, namely, substrate-assisted catalysis, in which the substrate itself plays the role of the general base and extracts a proton from the attacking water molecule, has also been proposed.[6,9] However, most of the mechanistic studies were done with implicit water models (dielectric continuum) or with only one or two explicit water molecules (microsolvation approach), meaning some reaction pathways and certainly solvent effects were often all but excluded. Those with only one explicit water naturally favored substrate-assisted catalysis *a priori*. Additionally, a large number of studies concentrated mainly on smaller molecules, for example, monophosphates, pyrophosphates, phosphomonoesters, phosphodiesters, etc., which are possibly not optimal models for triphosphate systems.

SYSTEM SETUP AND METHODS

This work investigates the reaction mechanism of phosphate hydrolysis in solution using accelerated *ab initio* molecular dynamics simulations,[24] as explained in more detail in the Supporting Information. As the guanine base of GTP is of little importance for the hydrolysis reaction in solution, the model system was chosen to comprise a fully deprotonated methylated triphosphate molecule ($MeTP^{4-}$, see the inset in Figure 1) plus a magnesium cation solvated in 113 water molecules, following the pioneering work of ref 11 (see structure 1N in Figure 2a and structure (a) in Supporting Figure 2).

Received: October 28, 2011
Published: April 3, 2012

dx.doi.org/10.1021/ja2101533 | J. Am. Chem. Soc. 2012, 134, 6995−7000

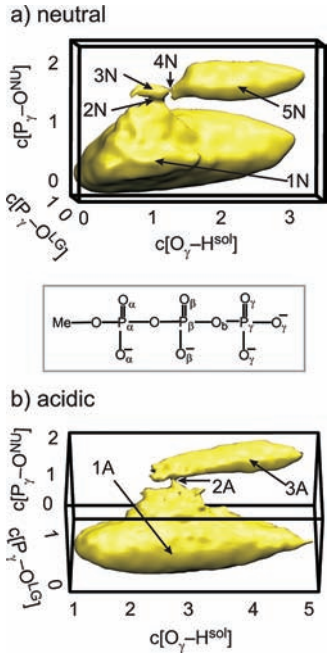

Figure 1. Free energy surfaces obtained for the neutral (a) and acidic (b) hydrolysis reactions marking and labeling the extrema, which are depicted in Figure 2. The surfaces have been smoothed for visualization purposes; both isosurfaces were plotted at a value of 29 kcal/mol. The middle inset shows the initial structure for the simulations, i.e., the fully deprotonated MeTP^{4-} species, including the naming of its relevant atoms.

To ascertain the effect of a change in pH, another simulation was set up using the same system as above, except for the addition of two excess protons to yield a strongly acidic pH (see structure (b) in Supporting Figure 2). In the *ab initio* metadynamics simulations,[25−27] we computed the FES within a chemically relevant "reaction subspace" spanned by the following three so-called collective variables, which were constructed so as to cover all aforementioned reaction mechanisms: (i) the coordination number of the γ-phosphate to the two β-oxygens and the bridging oxygen (O_b), (ii) the coordination number of the γ-phosphate to all water oxygens, and (iii) the coordination number of all three γ-oxygens and O_b to all water hydrogens in the system (see the inset in Figure 1 and Supporting Information for details). To get a better idea of the chemistry behind the reaction mechanisms and, in particular, changes in charge states, the electronic structure was analyzed in terms of maximally localized Wannier functions.[28]

RESULTS AND DISCUSSION

The relevant structures and, ultimately, reaction mechanisms extracted from analyzing the FESs are shown in Figure 2a and b for the hydrolysis of MeTP into MeDP and inorganic phosphate (P_i) under neutral (N) and acidic (A) conditions. The three-dimensional FESs themselves are depicted in Figure 1 for both cases. Generally speaking, there are two main differences: on the one hand, there is the formation of a possible transient intermediate (or "flat TS", *vide infra*) in the neutral case, which does not appear on the acidic FES (see Figure 3), and on the other hand, there are two distinct reaction mechanisms which differ by the protonation of one of the γ-oxygens in the acidic TS.

In a detailed analysis of the neutral case, the global minimum on the FES is represented by a deprotonated reactant, MeTP^{4-}, which coordinates the Mg^{2+} ion octahedrally with one of its β and one of its γ-oxygens together with four water molecules; see structure 1N in the left panel of Figure 2. The initial barrier of ca. 29 kcal/mol (which corresponds to a thermal energy of roughly 50 k_BT at ambient conditions) represents the breakage of the γ-phosphate to bridging oxygen bond and the positioning of the attacking water molecule (structure 2N) leading to the formation of a very shallow intermediate on the FES at around 27 kcal/mol, which lies just within the limitations of our sampling accuracy (see Supporting Information). This intermediate (structure 3N) constitutes a planar, symmetrical metaphosphate ion, PO_3^-, which remains sandwiched between the MeDP^{3-} leaving group (LG) and the water nucleophile (Nu). Note that the charge states assigned here and later are based solely on the outcome of the Wannier analysis of the periodic system's electronic structure. The next barrier of ca. 2 kcal/mol (roughly 3 k_BT) corresponds to the addition of the nucleophilic water molecule to the PO_3^- moiety (structure 4N), leading to the final products of an $H_2PO_4^-$ ion and a MeDP^{3-} molecule (structure 5N). Mechanistically speaking, the role of a general base is assumed by a second "assisting" solvation water molecule, which arranges itself via the hydrogen bond network in the vicinity of the attacking nucleophile water and accepts a proton to form an H_3O^+ ion; the assisting water is marked with an asterisk in Figure 2a. This generates an OH^- species that simultaneously attacks the phosphorus atom of PO_3^- and forms a new bond while the leaving group departs, resulting in an HPO_4^{2-} ion and the hydronium ion. The very proton transferred from the attacking water to the assisting water is then donated almost immediately from the hydronium ion to one of the HPO_4^{2-}-oxygens in a rather cyclic fashion, yielding the final $H_2PO_4^-$. This means that the second proton emanates from the same water molecule that supplied the nucleophile, whereas the assisting water molecule leaves the scene intact. Such a complex reactive solvation scenario is difficult to probe using microsolvation approaches. The complete reaction thus follows a $D_N{*}A_ND_{xh}A_H$ mechanism; see refs 29 and 30 for definitions. According to this IUPAC nomenclature, $D_N + A_N$ would represent a long-lived intermediate, and D_NA_N implies the existence of a distinct TS, whereas $D_N{*}A_N$ indicates a shallow intermediate or "flat TS". Note in passing that the free energy of activation is consistent with the experimental value of 28 kcal/mol at neutral conditions;[31] previous theoretical results for MeTP hydrolysis in neutral solution range from 20 to 35 kcal/mol.[11,13,14]

In acidic solution, things are somewhat different even though the collective variables chosen were identical to those in the neutral system. The reactant global minimum was represented by two structures that differ in their protonation state; see the structure examples labeled 1A and 1A′ in Figure 2b. The reactant was protonated either once or twice, thereby generating a MeTPH^{3-} and an MeTPH$_2^{2-}$ species, respectively, whereby a γ-oxygen was always protonated and a β-oxygen was protonated in several structures but not in all of them. These different structures with similar values of collective variables make up part of the configurational entropy of the system. More significantly, the intermediate observed in the neutral case was absent on the acidic FES, leaving instead just a first-order saddle point at around 29−30 kcal/mol, corresponding to about 50 k_BT.

The TS in the acidic case (structure 2A in Figure 2b) represents a complex process, namely, (i) the breaking of the P_γ−O_{LG} bond, (ii) the making of the bond to the incoming nucleophile, (iii) its deprotonation by an assisting water (marked with an asterisk in the Lewis formula), and (iv) the

dx.doi.org/10.1021/ja2101533 | J. Am. Chem. Soc. 2012, 134, 6995−7000

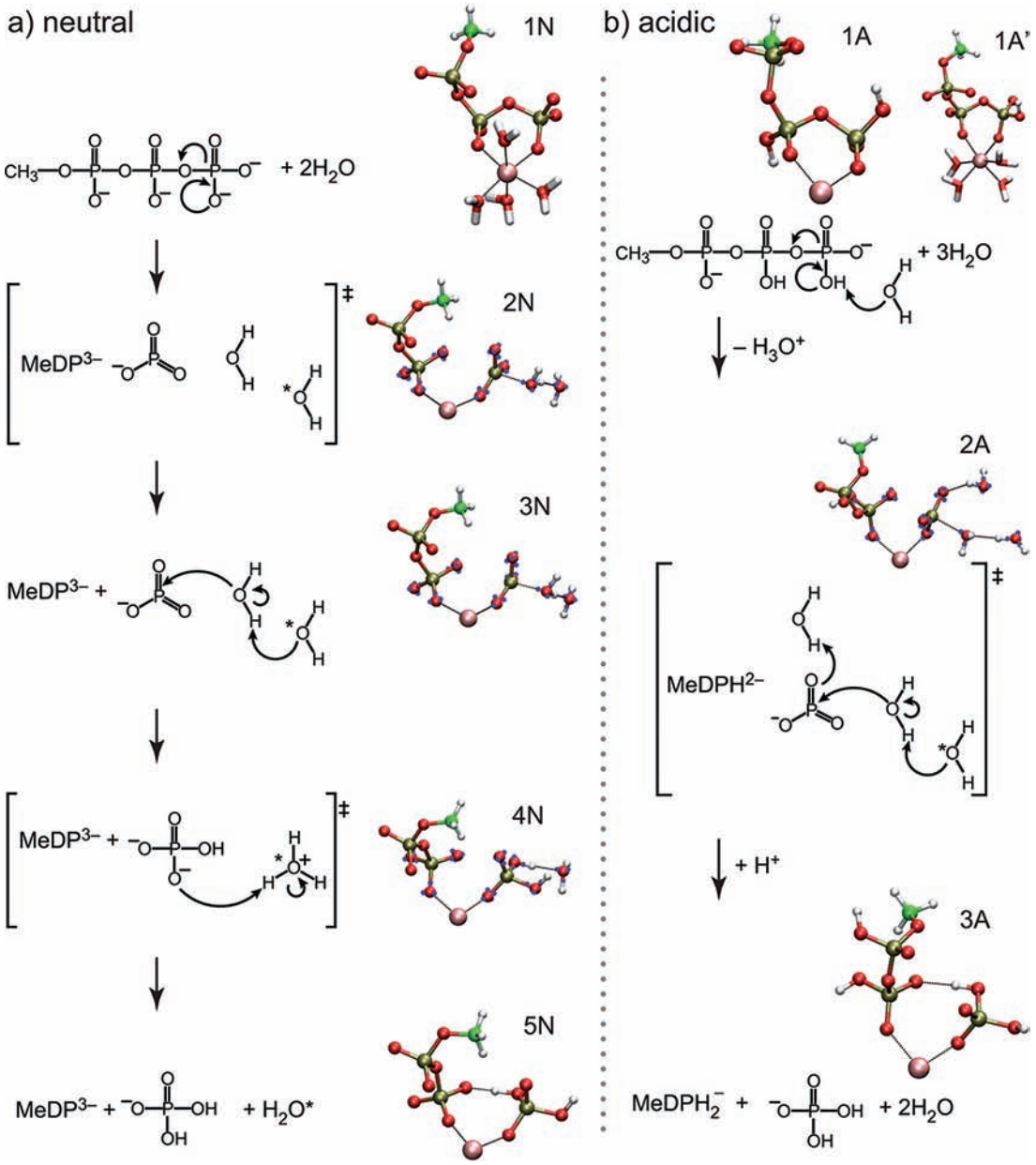

Figure 2. Sampled configurations (ball-and-stick) and schematic representations (note: arrows strictly indicate electron pair movement) based upon the FESs of the hydrolysis mechanism in neutral (a) and acidic (b) solution showing all intermediates and transition states using the same labeling as in Figure 1. Bulk water molecules are omitted for clarity (O, red; H, white; P, bronze; C, green; Mg^{2+}, pink) and the oxygen of the assisting water molecule is marked by an asterisk in both cases. The Wannier centers representing the localized orbitals and used to determine the charge state of the atoms in the schematic mechanisms are marked by blue spheres and are shown only in the reacting species for clarity. The first full octahedral coordination shell of Mg^{2+} is shown soley in structures 1N and 1A′, and in panel b, the Lewis structures have been depicted only for structure 1A.

reorganization of a water molecule to protonate the γ-oxygen. Overcoming this activation barrier leads therefore directly to the final products of protonated MeDP ($MeDPH_2^-$) and an $H_2PO_4^-$ ion (structure 3A). Mechanistically, the deprotonation of the attacking water proceeds once again through a second solvation water; however, in this case, it occurs simultaneously with the protonation of one of the γ-oxygens of the PO_3^- moiety. The free nucleophilic OH^- ion formed can now attack the γ-phosphate to give the final products. The hydrogen ion that protonates the γ-oxygen emanates from a Zundel complex formed in the surrounding solution, *ergo* from a different water molecule to the one that acted as the nucleophile. The $MeDPH_2^-$ species formed in the product is protonated twice, and the second proton now does originate from the water molecule that attacks the PO_3^- moiety. As nucleophilic attack and protonation occur simultaneously here, this part of the reaction is an example of concerted general acid-catalyzed hydrolysis, which follows an $A_NA_HD_{xh}$ mechanism. The entire mechanism is thus described as $D_NA_NA_HD_{xh}$.

Closer examination of the reaction mechanisms extracted from our metadynamics simulations reveals that they exhibit both dissociative and associative characteristics. Several observables can help to define the nature of a TS or intermediate, for example, the $P\gamma-O_{LG}$ and $P\gamma-O_{Nu}$ bond lengths or the change in atomic charges along the minimum free energy pathway (MFEP). Table 1 shows the average γ-

dx.doi.org/10.1021/ja2101533 | J. Am. Chem. Soc. 2012, 134, 6995–7000

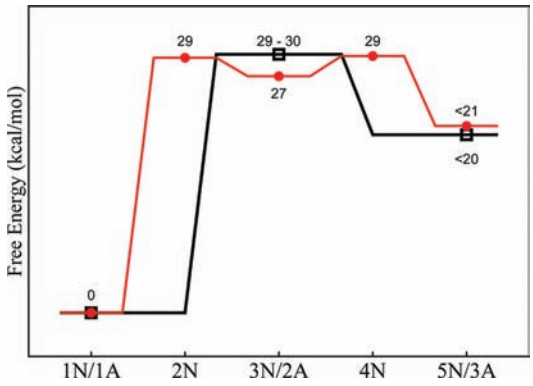

Figure 3. Schematic free energy profiles in acidic (A) solution (black line) and in neutral (N) solution (red line) representing the minimum free energy pathways extracted from the FESs shown in Figure 1. The extrema along the pathway (here, abscissa) correspond to the structures defined in Figure 2, whereby structures 1N–5N concur with the neutral system and structures 1A–3A with the acidic system.

Table 1. Average Bond Lengths and Pγ Mulliken Charges for the Acidic and Neutral MFEP Structures and Their Standard Deviations[a]

structure	$P\gamma-O_{LG}$ (Å)	$P\gamma-O_{Nu}$ (Å)	Pγ charge
1A	1.72 ± 0.14	5.90 ± 0.41	1.49 ± 0.14
2A	2.69 ± 0.02	2.28 ± 0.01	1.62 ± 0.01
3A	3.42 ± 0.10	1.65 ± 0.04	1.48 ± 0.05
1N	1.68 ± 0.08	5.68 ± 0.67	1.53 ± 0.08
2N	3.11 ± 0.01	2.03 ± 0.02	1.70 ± 0.01
3N	3.06 ± 0.01	1.95 ± 0.01	1.74 ± 0.02
4N	3.26 ± 0.01	1.66 ± 0.01	1.59 ± 0.01
5N	3.42 ± 0.23	1.64 ± 0.05	1.50 ± 0.09

[a] The labels correspond to the structures defined in Figure 2. Note: all structures within 1 k_BT of the extrema found on the FESs were taken into account and used to compute the error bars.

phosphate to bridging oxygen (LG) bond length and its average distance to the attacking water oxygen (Nu) for the representative structures found along the acidic and neutral MFEPs. In both reactions, the bond to the LG is broken before the Nu has fully added onto the moiety; however, as the bond to the Nu is partially formed in both cases, it also indicates that interaction with the nucleophile is important for the ionization of the substrate in the first place. The large amount of bond cleavage to the $MeDP^{3-}$ LG in the neutral intermediate makes it reminiscent of an S_N1 carbocation-like intermediate, but as a result of the Nu participation mentioned above, the substrate remains a contact ion pair (CIP) and the PO_3^- cannot dissociate away into the surrounding solution. A true stepwise S_N1 mechanism, in which no covalent interaction between the substrate and nucleophile is required for the intermediate to dissociate, would form a solvent-shared or fully solvated IP and a long-lived intermediate on the FES. Here, as the nucleophile is needed for formation of the intermediate, the reaction proceeds via a coupled S_N1 mechanism on a CIP. On the other hand, the existence of a distinct TS on the acidic FES means that the mechanism is shifted even more toward the associative S_N2 limiting case. The TS formed in this reaction resembles an "exploded" S_N2 TS, which although structually very similar to the shallow intermediate described above represents a distinct saddle point on the FES.

Another characteristic that distinguishes between an S_N2 and a S_N1 regime is the amount of charge (transfer) on the three main atoms, here P_γ, O_{LG}, and O_{Nu}. In all variations of an S_N1 mechanism, there is a net positive charge (electron deficiency) at the phosphorus atom, in the S_N2 limit, however, this charge becomes more negative.[32] To this end, we examined the average Mulliken charges of the γ-phosphate for all of the structures obtained from the MFEPs; see Table 1. As one can see, the charge on the phosphorus increases in both cases as the reaction proceeds from the reactants through the TS or intermediate and decreases again as the product is formed. This increase in the electrophilicity of the reactive center in the acidic reaction is less pronounced, but nevertheless these results suggest that although the intermediate or TS formed is similar in structure to an S_N2 one, we are still within the S_N1 regime in both cases, in which the phosphorus atom becomes more electronegative as the TS is formed. This means that the bond to the LG is broken before the bond to the Nu is formed withdrawing even more electron density from the already electrophilic phosphorus. In a true S_N2 regime, the phosphorus would become more negative as the Nu provides electron density in the form of a new bond before the LG has departed.

A complementary way to analyze the nature of a reactive intermediate is through use of a More O'Ferrall-Jencks (MOFJ) plot,[33] which correlates the evolution of $P_\gamma-O_{LG}$ bond cleavage and $P_\gamma-O_{Nu}$ bond formation. The corners of the plot represent the local minima, i.e., reactants, products, and the two possible "ideal" intermediates. Note that the $P_\gamma-O_{LG}$ distance is closely related to the first collective variable and the $P_\gamma-O_{Nu}$ distance is related to the second collective variable; thus, the MOFJ plot correlates directly to the free energy landscapes depicted in Figure 1. According to Figure 4, both neutral and acidic

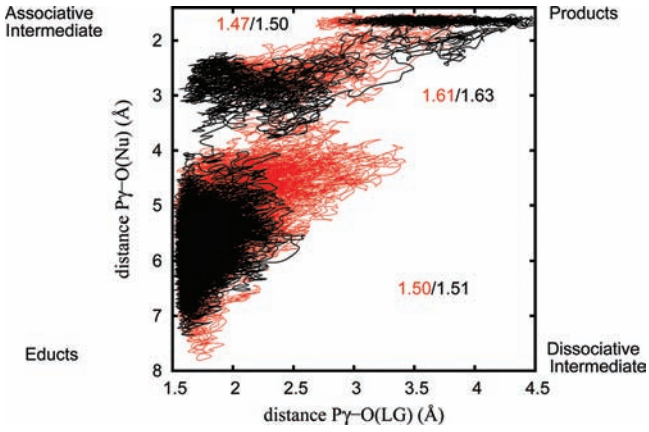

Figure 4. More O'Ferrall-Jencks plot for the reaction pathways in acidic solution (black line) and in the neutral solution (red line); the corresponding average Mulliken charges for each "basin" are given within the plot using the same color scheme.

reactions lie nearer to the associative pathway than the dissociative pathway. However, the sampling of the possible intermediate in the neutral case can clearly be seen as a lengthening of the $P_\gamma-O_{LG}$ bond when comparing the neutral to the acidic MOFJ plot. Additionally, the average Mulliken charges of the γ-phosphate were calculated for each basin; see Figure 4. The charges endorse the results based on the MFEP structures (see Table 1) and support the notion that, despite the S_N2-like structure of the TS or intermediate, we are still within the S_N1 regime for both reactions. An excerpt of the

dx.doi.org/10.1021/ja2101533 | J. Am. Chem. Soc. 2012, 134, 6995–7000

evolution of the $P_\gamma-O_{LG}$ and $P_\gamma-O_{LG}$ bond distances along the metadynamics trajectory underlying these MOFJ plots is shown in Figure 9 in the Supporting Information. Figures 10 and 11 in the Supporting Information also show the change in Mulliken charges for the main atoms, i.e., P_γ, O_{LG}, and O_{Nu}, as they progress along the trajectories.

According to ref 3, an increase in nucleophile participation in a substitution reaction depends on the stability of the intermediate itself. Such unstable intermediates that react with a neighboring nucleophile faster than they can diffuse away tend to interact through a preassociation mechanism. The reactants have to be assembled through an encounter complex before bond making or breaking can occur. This transient complex contains elements of all of the reactants in it, in this case MeDP, PO_3^-, and a water molecule. It is highly probable that the rearrangement of the bulk solvent to promote assembly of this encounter complex contributes to the high activation barrier of both reactions. The Mg^{2+} ion coordinates a β-oxygen in the LG and a γ-oxygen in the PO_3^- intermediate throughout all simulations, holding them together in some respect, preventing the intermediate from dissociating through the bulk solvent. Consequently, the role of the Mg^{2+} ion could be not only to accelerate the reaction by increasing the electrophilicity of the phosphorus atom[34] but additionally to assist the formation of the encounter complex by electrostatic interactions to the PO_3^- and the LG, thereby lowering its activation energy. The (Walden) inversion of configuration observed at the phosphorus center in all simulations supports the view of an preassociation mechanism.[32,35] It is usually a trait of an S_N2 mechanism, leading to second order reaction kinetics; however, nucleophilic attack on a CIP also leads to a complete configurational inversion as the nucleophile is only able to attack the intermediate from one side as the LG shields the other side. A free, solvated metaphosphate S_N1 intermediate could be attacked by the Nu on both sides.

SUMMARY AND OUTLOOK

This work discloses the detailed hydrolysis mechanisms of a model nucleoside triphosphate in acidic and neutral solution by means of accelerated *ab initio* simulations that sample a large configurational space that fully includes the reactive solvent. Both hydrolyses are found to proceed via different mechanisms: the acidic system reacted by means of concerted general acid catalysis, i.e., a $D_NA_NA_HD_{xh}$ mechanism, whereas the neutral system reacted by way of a $D_N{*}A_ND_{xh}A_H$ mechanism. Despite this classification, both mechanisms are not clear-cut and we cannot present our results "in a nutshell", which however readily explains the conflicting conclusions in the literature. All of the evidence from the simulations points toward a coupled S_N1 mechanism with a short-lived intermediate on the FES at neutral pH with a transition to a loose, "exploded" S_N2 TS at acidic pH. Although the existence of the intermediate is at the limit of the accuracy of the calculations, the mechanisms are clearly distinguished by the simultaneous protonation of the γ-oxygen in the acidic PO_3^- moiety, regardless of whether a shallow intermediate or a "flat TS" was formed on the FES. This protonation is a phenomenon frequently observed in reactions that take place in acidic solution. The nucleophile is needed for PO_3^- dissociation in both cases and because of the instability or nonexistence of the intermediate, formation of a preassociation complex is a prerequisite for the reaction to occur. This may be facilitated by the Mg^{2+} ion. It is not a true S_N2 (associative) mechanism as the bond to the LG is broken before the bond to the incoming Nu is formed. This leads to increased electron deficiency at the reactive center, which is characteristic of an S_N1 (dissociative) regime. The part of a general base was played by another, assisting water molecule in both systems, which has not been seen before. Interestingly, substrate-assisted catalysis was not observed in the bulk water environment. On the basis of these findings, the same simulation approach holds great promise to shed light on the even more demanding enzymatic hydrolysis mechanism in GTPase proteins.

ASSOCIATED CONTENT

Supporting Information

Computational details describing the exact setup of the simulations, including a discussion of the parameters employed, as well as additional data from the underlying metadynamics trajectories. This material is available free of charge via the Internet at http://pubs.acs.org.

AUTHOR INFORMATION

Corresponding Author

rachel.glaves@theochem.rub.de

Present Address

[†]Lehrstuhl für BioMolekulare Optik, Ludwig-Maximilians-Universität München, Oettingenstr. 67, 80538 München, Germany.

Notes

The authors declare no competing financial interest.

ACKNOWLEDGMENTS

We are indebted to Nisanth Nair and Harald Forbert for many stimulating discussions and technical help. R.G. gratefully acknowledges a doctoral fellowship from the "Ruhr University Research School" RURS (DFG GSC/98). The calculations were carried out at the Leibniz-Rechenzentrum Supercomputer HLRB-II and in parts at SuperMUC (Munich) as well as at Bovilab@RUB (Bochum).

REFERENCES

(1) Krauss, G. *Biochemistry of Signal Transduction and Regulation*; Wiley & Sons: New York, 2001.

(2) Bowler, M. W.; Cliff, M. J.; Waltho, J. P.; Blackburn, G. M. *New J. Chem.* **2010**, *34*, 784−794.

(3) Jencks, W. P. *Acc. Chem. Res.* **1980**, *13*, 161−169.

(4) Westheimer, F. H. *Chem. Rev.* **1981**, *81*, 313−326.

(5) Hengge, A. C.; Edens, W. A.; Elsing, H. *J. Am. Chem. Soc.* **1994**, *116*, 5045−5049.

(6) Florián, J.; Warshel, A. *J. Am. Chem. Soc.* **1997**, *119*, 5473−5474.

(7) Florián, J.; Warshel, A. *J. Phys. Chem. B* **1998**, *102*, 719−734.

(8) Aqvist, J.; Kolmodin, K.; Florián, J.; Warshel, A. *Chem. Biol.* **1999**, *6*, 71−80.

(9) Admiraal, S. J.; Herschlag, D. *J. Am. Chem. Soc.* **2000**, *122*, 2145−2148.

(10) Wang, Y. N.; Topol, I. A.; Collins, J. R.; Burt, S. K. *J. Am. Chem. Soc.* **2003**, *125*, 13265−13273.

(11) Akola, J.; Jones, R. O. *J. Phys. Chem. B* **2003**, *107*, 11774−11783.

(12) Boero, M.; Ikeda, T.; Ito, E.; Terakura, K. *J. Am. Chem. Soc.* **2006**, *128*, 16798−16807.

(13) Grigorenko, B. L.; Rogov, A. V.; Nemukhin, A. V. *J. Phys. Chem. B* **2006**, *110*, 4407−4412.

(14) Klähn, M.; Rosta, E.; Warshel, A. *J. Am. Chem. Soc.* **2006**, *128*, 15310−15323.

(15) Kamerlin, S. C. L.; Williams, N. H.; Warshel, A. *J. Org. Chem.* **2008**, *73*, 6960−6969.

(16) Rosta, E.; Kamerlin, S. C. L.; Warshel, A. *Biochemistry* **2008**, *47*, 3725−3735.
(17) Ruben, E. A.; Plumley, J. A.; Chapman, M. S.; Evanseck, J. D. *J. Am. Chem. Soc.* **2008**, *130*, 3349−3358.
(18) Kamerlin, S. C. L.; Florián, J.; Warshel, A. *Chem. Phys. Chem.* **2008**, *9*, 1767−1773.
(19) Kamerlin, S. C. L.; Haranczyk, M.; Warshel, A. *Chem. Phys. Chem.* **2009**, *10*, 1125−1134.
(20) Tang, E.; Tommaso, D. D.; de Leeuw, N. H. *J. Chem. Phys.* **2009**, *130*, 234502.
(21) López-Canut, V.; Roca, M.; Bertrán, J.; Moliner, V.; Tuñón, I. *J. Am. Chem. Soc.* **2010**, *132*, 6955−6963.
(22) Yamamoto, T. *Chem. Phys. Lett.* **2010**, *500*, 263−266.
(23) Branduardi, D.; De Vivo, M.; Rega, N.; Barone, V.; Cavalli, A. *J. Chem. Theory Comput.* **2011**, *7*, 539−543.
(24) Marx; D. Hutter, J. *Ab initio Molecular Dynamics: Basic Theory and Advanced Methods*; Cambridge University Press: New York, 2009.
(25) Laio, A.; Parrinello, M. *Proc. Natl. Acad. Sci. U.S.A.* **2002**, *99*, 12562−12566.
(26) Iannuzzi, M.; Laio, A.; Parrinello, M. *Phys. Rev. Lett.* **2003**, *90*, 238302.
(27) Laio, A.; Gervasio, F. L. *Rep. Prog. Phys.* **2008**, *71*, 126601.
(28) N. Marzari, N.; Vanderbilt, D. *Phys. Rev. B* **1997**, *56*, 12847−12865.
(29) Guthrie, R. D. *Pure Appl. Chem.* **1989**, *61*, 23−56.
(30) R. D. Guthrie, R. D.; Jencks, W. P. *Acc. Chem. Res.* **1989**, *22*, 343−349.
(31) Kötting, C.; Gerwert, K. *Chem. Phys.* **2004**, *307*, 227−232.
(32) Carey, F. A.; Sundberg, R. J. *Advanced Organic Chemistry: Structure and Mechanisms*; Springer: New York, 2007.
(33) Harris, J. M.; Shafer, S. G.; Moffatt, J. R.; Becker, A. R. *J. Am. Chem. Soc.* **1979**, *101*, 3295−3299.
(34) Franzini, E.; Fantucci, P.; de Gioia, L. *J. Mol. Catal. A: Chem.* **2003**, *204*−*205*, 409−417.
(35) van Bochove, M. A.; Swart, M.; Bickelhaupt, F. M. *Phys. Chem. Chem. Phys.* **2009**, *11*, 259−267.